A powerful two-dimensional chromatography method for the non-target analysis of depolymerised lignin

Eliise Tammekivi, Magali Batteau, Dorothée Laurenti, Hugo Lilti, Karine Faure

A powerful two-dimensional chromatography method for the non-target analysis of depolymerised lignin

Eliise Tammekivi[a], Magali Batteau[a], Dorothée Laurenti[b], Hugo Lilti[b], Karine Faure[a]*

[a]Universite Claude Bernard Lyon 1, ISA UMR 5280, CNRS, 5 rue de la Doua, 69100 Villeurbanne, France

[b]Universite Claude Bernard Lyon 1, IRCELYON UMR 5256, CNRS, 2 Av. Albert Einstein, 69626 Villeurbanne, France

*Corresponding author: karine.faure@isa-lyon.fr, Phone number 0437423686

Abstract

Background: Lignin is an abundant natural polymer obtained as a by-product from the fractionation of lignocellulosic biomass. In the name of a circular economy, lignin should be valorised into valuable chemicals or biomaterials and utilised instead of petrochemicals. For the development of efficient valorisation processes, the structural characterisation of lignin can be highly beneficial. However, this is an arduous task, as the isolated (and sometimes processed) lignin mainly consists of various neutral monomers but also oligomers. In addition, the material contains isomers, which can be especially problematic to separate and identify.

Results: We present a powerful off-line comprehensive two-dimensional (2D) chromatography method combining liquid chromatography (LC), supercritical fluid chromatography (SFC), and high-resolution mass spectrometry for the non-target analysis of depolymerised lignin. The implementation of a 1-aminoanthracene column in the second dimension enabled a class separation of potential lignin monomers, dimers, trimers, and tetramers with an additional separation based on the number of hydroxyl groups and steric effects. The pentafluorophenyl column in the first dimension additionally improved the separation based on hydrophobicity. The comparison of off-line 2D LC×SFC to 1D SFC showed that besides the overall improved performance, the first method is also superior for the separation of isomers. Advanced data analysis methods (MS-DIAL, SIRIUS, and Feature-Based Molecular Network) were integrated into the non-target workflow to rapidly visualise and study the detected compounds, which proved to be especially beneficial for the characterisation of the separated isomers.

Significance: The method yielded the first 2D LC plot demonstrating a classification of lignin compounds, which can be applied to compare various lignin sources and processing methods. In addition, the technique demonstrated improved separation of compounds, including isomers, which was especially beneficial as 77% of the detected compounds had at least one isomer in the same lignin sample.

Abbreviations: ^{1}D, ^{2}D: first and second dimension, respectively; 1D, 2D: one-dimensional and two-dimensional chromatography, respectively; MN: molecular network; FBMN: feature-based molecular network; HRMS: high resolution mass spectrometry; DDA: data-dependent acquisition; DIA: data-independent acquisition; MtBE: methyl *tert*-butyl ether; DEA: diethylamine; 1-AA: 1-aminoanthracene; BPC: base peak chromatograms; EIC: extracted ion chromatograms; GNPS: Global Natural Products Social Molecular Networking; DBE: Double Bond Equivalent; log*P*: octanol-water partition coefficient

1. Introduction

Lignin is an abundant natural polymer that is by far the largest natural resource for aromatic compounds. Nevertheless, it is considered to be a low-value residue and is largely burned to power the pulp and paper industry, where lignin is obtained by the fractionation of cellulose from lignocellulosic biomass.[1] However, due to the legislations to decrease carbon dioxide emissions, there is an increasing demand to use less petroleum and petrochemicals by replacing them with alternative natural resources. One alternative could be lignin, as it has potential to be valorised into valuable aromatic compounds (e.g., vanillin, phenol), by incorporating them into materials (e.g., coatings, resins, thermoplastics, battery electrodes), or transformed into additives for biofuel.[1,2] As the first step in the pulp or cellulosic ethanol industry, lignin is separated from the lignocellulosic biomass, which also contains cellulose and hemicellulose. Depending on the final aim and valorisation process, the isolated lignin can be depolymerised to a varying extent into smaller oligomers and/or monomers.[3] However, for constructing efficient valorisation processes, thorough structural characterisation of the product and/or intermediates can be highly beneficial.[1,4]

Structurally, the polymeric lignin consists of randomly coupled three aromatic subunits (syringyl, guaiacyl, and *p*-coumaryl) which, most commonly, are connected through β-O-4, β-5, β-β, 5-5, or 5-O-4 linkages (Figure 1). The proportions of the monomeric subunits as well as the amount and type of the linkages depend on the botanical origin of the lignin, thus yielding lignin polymers with highly varying structures. In addition, largely because of the reactive hydroxyl groups that can lead to condensation and repolymerisation, it is very difficult to isolate lignin without inducing modifications in the structure. Therefore, because of the variety in the original structure, the influence of the fractionation process, and variations in depolymerisation, the structural analysis of lignin and products is highly challenging.[3]

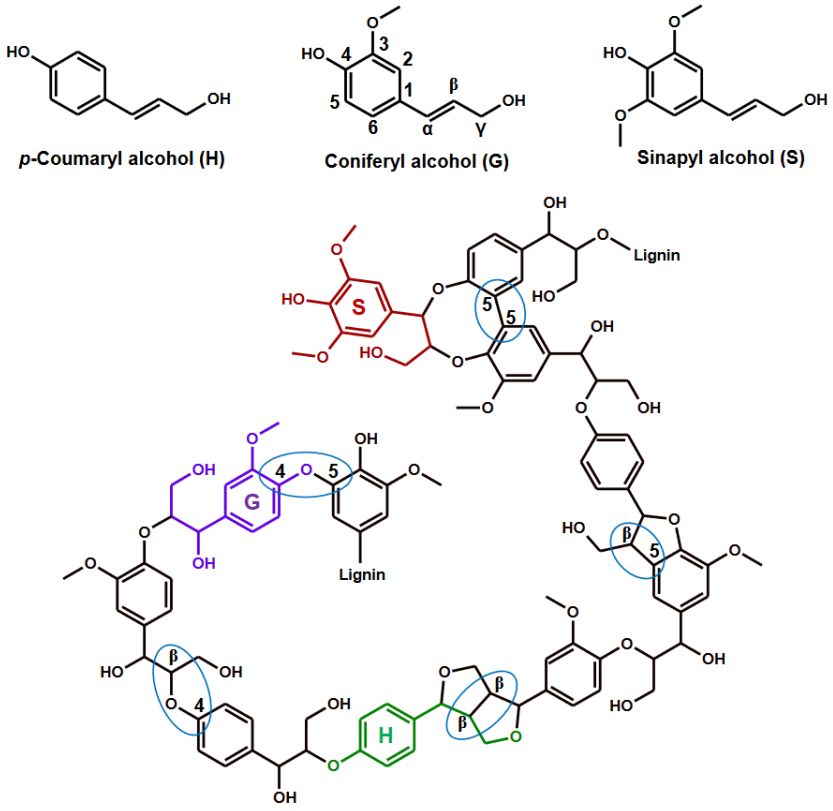

Figure 1. An exemplary partial lignin structure and its main units – *p*-coumaryl (H, green), guaiacyl (G, purple), and syringyl (S, red) shown in the structure. Examples of the main linkages (β-O-4, β-5, β-β, 5-5, 5-O-4) are highlighted by blue ovals. Above the lignin structure are the main subunits that by radical coupling form the lignin structure.[3,5]

One widely used method that can aid with obtaining detailed structural information about the depolymerisation products is chromatography. Because of the complex structure of depolymerised lignin, two-dimensional (2D) chromatography is applied more and more, as it has demonstrated higher peak capacity and improved selectivity compared to one-dimensional (1D) chromatography.[6–8] 2D gas chromatography (2D GC, largely as GC×GC) is nowadays considered to be a standard method for the analysis of processed biomass.[9] However, with 2D GC commonly only lignin monomers and dimers are detected, as larger oligomers are not volatile enough for GC.[4,7] Volatility is less of an issue with liquid chromatography (LC) and, indeed, 2D LC has been successfully applied for the analysis of poorly volatile or thermally unstable compounds, such as carotenoids[10] or bioactive polyphenols[11]. However, 2D LC has been much less applied for the analysis of biomass, as it is often problematic to hyphenate two LC dimensions having non-correlated separation mechanisms (in other words, high orthogonality) such as NPLC×RPLC.[4] In the case of depolymerised lignin, the sample generally consists of neutral compounds, for which 2D LC methods combining reversed-phase LC (RPLC) and supercritical fluid chromatography (SFC) have demonstrated good orthogonality.[12] The studies by Sun *et al*.[6] and Sarrut *et al*.[13] have already demonstrated some first advantages of applying LC×SFC for the analysis of monomeric neutral compounds. However, to obtain more information about the separation and detected compounds, mass spectrometry (MS) detection is compulsory. Together with fragmentation, high resolution MS (HRMS) is an indispensable tool to perform non-target analysis, where the aim is to detect and annotate essentially as many analytes as possible without a prior analyte selection. Currently, only a small proportion of the compounds can be identified, as the non-target acquisition and data analysis remain a challenge.[14] Applying 2D separation before the MS detection can be highly beneficial, as the improved separation will reduce the complexity caused by the number of co-eluting ions and at the same time decrease ion suppression, thus improving ionisation. These aspects can lead to identification with higher confidence, detection of minor components, and a more reliable quantification when suitable standards are available.[15]

For efficient and repeatable data analysis, more and more computational tools are emerging. In this work, we applied MS-DIAL[16] for peak picking, MS/MS deconvolution, peak alignment, and cleaning of the MS/MS spectra. This software can use both data-dependent acquisition (DDA) and data-independent acquisition (DIA) data as the input, which, after treatment, can be straightforwardly exported in a format suitable for the Molecular Network (MN) analysis. The Global Natural Products Social Molecular Networking (GNPS) platform organises detected features together based on their MS/MS spectral similarities.[17] This has proven to be a powerful approach for the discovery of novel components also in natural products.[18] In recent years, the combined utilisation of 2D LC and MN for the non-target analysis of natural products has increased. One of the major areas is the analysis of traditional Chinese medicine using off-line methods combining RPLC with NPLC, HILIC, or mix-mode LC.[19–22] As far as we know, Qu *et al*.[23] and Wei *et al*.[24] have been the only ones to apply off-line LC×SFC together with MN for the analysis of complex samples, in their case, traditional Chinese medicine. However, in our work, we collected approximately three times more fractions from the first dimension (^{1}D) to decrease the under-sampling effect that substantially decreases the effective peak capacity of an off-line 2D method.[25]

In the present study, the aim was to apply a powerful off-line comprehensive LC×SFC-HRMS/MS method for the non-target analysis of depolymerised lignin, which also includes oligomers higher than dimers. Particular focus was given to the separation and study of isomers with MN, as depolymerised lignin is expected to contain a high number of isomers. To our knowledge, this is the first study to combine a comprehensive 2D LC method with MS and apply it to the analysis of lignin.

2. Materials and methods

2.1 Chemicals and sample preparation

LC-MS grade methanol (MeOH) and methyl *tert*-butyl ether (MtBE) of HPLC grade were purchased from Sigma-Aldrich (Darmstadt, Germany), and formic acid (FA, 95-97%) from Aldrich. LC-MS grade acetonitrile (ACN) was purchased from Honeywell Riedel-de-Haën (Seelze, Germany) and pressurised liquid CO_2 (99.995%) from Air Liquide (Pierre Bénite, France). Water suitable for MS was produced by using an Elga water purification system (Veolia water STI, Le Plessis Robinson, France).

Based on previously published studies,[6,26–28] 33 phenolic standards were selected to represent monomeric compounds that can be produced from lignin depolymerisation. All the following standards were purchased from Sigma-Aldrich (with numbering corresponding to Table S1 in the Supplementary Information - SI): anisole (1); 2,3-benzofuran (2); 2,3-dihyrobenzofuran (3); eugenol (4); 2,4,6-trimethylphenol (5); 2,6-dimethylphenol (6); 2-phenylethanol (7); *trans*-isoeugenol (8); syringol (9); 2,5-dimethylphenol (10); 2-ethylphenol (11); *o*-cresol (12); *m*-cresol (13); 4-ethylphenol (14); *p*-cresol (15); phenol (16); acetovanillone (17); 3,4-dimethylbenzoic acid (18); acetosyringone (19); syringaldehyde (20); 4-hydroxybenzaldehyde (21); 4-hydroxyacetophenone (22); coniferaldehyde (23); 4-methylcatechol (24); catechol (25); vanillyl alcohol (26); 4-hydroxybenzoic acid (27); hydroquinone (28); ferulic acid (29); *p*-coumaric acid (30); 3,4-dihydroxyphenylacetic acid (31); pyrogallol (32); and caffeic acid (33). Other characteristics of the standards are presented in Table S1 in the SI.

2.2 Sample preparation

From each monomer standard, single-compound stock solutions of 1 mg mL^{-1} in methanol were prepared and stored at 5 °C. From these stock solutions, five mix solutions containing five or six standards were prepared and diluted with MeOH with a final concentration of 0.1 mg mL^{-1} for each monomer. To ease the MS interpretation, the standards were divided into mixtures (A, B, C, D, E, and F) so that monomers having the same molecular formula were in different mix solutions (Table S1 in the SI).

The depolymerised lignin sample was prepared by the following procedure, which will be presented in more detail in future publications focusing on the catalytic depolymerisation of lignin. Previously dried SODA P1000 lignin was depolymerised in a batch reactor in the presence of a $CoMoS/Al_2O_3$ catalyst and isobutanol at 280°C and 60 bar. The bio-oil was recovered by solubilisation in tetrahydrofuran followed by filtration to remove the catalyst and evaporation of the solvents. The yielding solid mixture was separated into two fractions by solubilisation in acetone and precipitation of the heavier fraction with *n*-heptane. After centrifugation, the supernatant (lighter fraction) was recovered and evaporated to dryness. From this oily solid, a solution of 30 mg mL^{-1} was prepared in MeOH, sonicated for 10 min in an ultrasonic bath, and the supernatant was collected for the chromatographic analyses.

2.3 Apparatus

The screening of columns for the SFC dimension was carried out using an Agilent (Santa Clara, CA, USA) 1260 Infinity II UHPSFC system. A more detailed overview of the experimental conditions used for the screening of columns is presented in Table S2 in the SI. The following columns, a Torus DEA (diethylamine, 1.7 µm, 3 mm x 100 mm), a Torus DIOL (1.7 µm, 3 mm x 100 mm), a Torus 1-AA (1-aminoanthracene, 1.7 µm, 3 mm x 100 mm), and a CORTECS HILIC (1.6 µm, 2.1 mm x 50 mm) were purchased from Waters (Milford, MA, USA).

For the ^{1}D LC separation in the off-line LC×SFC analysis, an Agilent 1260 Infinity II HPLC system was used, equipped with a binary solvent delivery pump (G7111A), an autosampler (G7129A) with a 900 µL loop, a thermostated column compartment (G7116A, up to 90 °C), a diode array detector (DAD) with a 1 µL flow-cell (G7117C), and a fraction collector with a capacity of 120 fractions (G1364F), all

from Agilent Technologies. The dwell volume was determined experimentally to be 2.65 mL. The instrument was controlled by using the Agilent Openlab CDS Chemstation software. A Kinetex F5 column (5 µm, 4.6 mm x 150 mm) was purchased from Phenomenex (Torrance, CA, USA). The column geometry was selected to allow the collection of fractions with a reasonable volume to be handled. A miVac centrifugal vacuum concentrator (Genevac, Ipswich, UK) was used to evaporate the fractions to dryness. For the ^{2}D SFC separation, a Waters UPC^{2} system equipped with a binary solvent delivery pump, an autosampler with a 10 µL loop, a thermostated column compartment (up to 90 °C), a DAD with an 8.4 µL flow-cell, a backpressure regulator (BPR), and a make-up solvent pump all from Waters. The instrument was controlled by using Waters Empower CDS software. A 5 cm long Torus 1-AA column (1.7 µm, 3 mm x 50 mm) was purchased from Waters.

For the accurate-mass tandem mass spectrometry detection, an Agilent 6560 Ion Mobility Quadrupole Time-of-Flight (Q-ToF) instrument equipped with an Agilent Jet stream electrospray ionisation (ESI) source was used. Agilent MassHunter Qualitative Analysis 10.0 was used for the extraction of base peak chromatograms (BPC) and extracted ion chromatograms (EIC). The 2D plots of the off-line LC×SFC measurement were visualised by using a Matlab (Mathworks) code developed in-house by S. Heinisch and F. Rouvière.

2.4 Methods

2.4.1 Off-line 2D LC×SFC-Q-ToF-MS/MS conditions

The ^{1}D LC separation was performed using the Kinetex F5 column with H_2O containing 0.1 vol.% of FA (**A**) and ACN containing 0.1 vol.% of FA (**B**). The column temperature was 30 °C and the injection volume was 10 µL. The flow rate was 2.1 mL min^{-1} and the gradient was the following: 1% to 100% of **B** in 9.0 min, held at 100% of **B** for 0.77 min (one column dead time), decreased back to 1% of **B** in 0.77 min, and equilibrated for 3.58 min. The Agilent fraction collector enabled the collection of 120 fractions into chromatographic vials with 250 µL inserts every 0.085 min starting after the column dead time. Therefore, the fractions consisted of the effluent eluting during gradient time and dwell time. The variability induced by the collection process is around 1%. After collection, the fractions were evaporated to dryness. Then, a volume equivalent to the previously collected volume of MtBE was added to the residue and the vial was vortexed for a few seconds.

The ^{2}D SFC separation was performed using the 5 cm Torus 1-AA column with supercritical CO_2 (**A**) and methanol as co-eluent (**B**). The column temperature was 40 °C and the injection volume was 7 µL. The flow rate was 1.4 mL min^{-1}, which was determined as the maximum flow rate accessible at 50% of **B**. The gradient was the following: 5% to 50% of **B** in 3.6 min, decreased back to 5% of **B** in 0.2 min, and held for 1.0 min to equilibrate the column. The BPR temperature and pressure were set to 70 °C and 140 bar, respectively. The DAD signal was registered at 210 nm and 254 nm.

The ^{2}D SFC column was hyphenated to the MS by using the "*preBPR splitter with a sheath pump*" configuration, described in more detail by Guillarme *et al.*[29] MeOH, with a flow rate of 0.5 mL min^{-1}, was used as the make-up solvent. The ESI was performed in the negative ionisation mode under the following parameters: drying and sheath gas temperature 350 °C with a flow of 11 L min^{-1}, nebuliser pressure 40 psi, capillary voltage 3.5 kV, and fragmentor voltage 185 V. The range of 90-1700 *m/z* was set for the mass scan. All ions fragmentation (AIF) mode with two experiments – collision energy 0 eV and 20 eV – were applied, which led to HRMS data for both MS^{1} and MS^{2}, respectively. The acquisition rate was 3 spectra per second.

2.4.2 1D SFC-Q-ToF-MS/MS conditions

For the 1D SFC-Q-ToF-MS/MS analysis, the SFC method was modified to provide the optimal separation that a corresponding 1D method can give, therefore enabling a fair comparison between the 2D and 1D separation (see section 3.7). Therefore, the longer 10 cm Torus 1-AA column and a longer gradient time (30 min) were selected. Because of these changes, other modifications had to be made. As the slope of the separation was much lower, the analytes eluted at a lower final eluent concentration (35% instead of 50%). In addition, because of the increased pressure caused by the longer column, the flow rate had to be decreased to 1.0 mL min^{-1} corresponding to the maximum flow at 35% of co-eluent. Therefore, the following gradient was applied: 5% to 35% of **B** (MeOH) in 30.0 min, 35% to 5% of **B** in 0.5 min, and equilibrated for 2.2 min. The other aspects of the 1D analysis (instrumentation, MS parameters, etc.) were the same as in the ^{2}D SFC component of the off-line LC×SFC-HRMS analysis.

2.4.3 Advanced data analysis

For the more detailed non-target analysis, a combination of feature detection, visualisation, and annotation tools was applied. First, the raw Agilent MassHunter data files (.D) were converted to .ABF (Analysis Base File) format using ABFConverter (Reifycs Inc., Tokyo, Japan). The data was processed with MS-DIAL software version 4.9 (RIKEN Centre for Sustainable Resource Science, Kanagawa, Japan) using the AIF multiple collision energies option. The mass tolerance was set at 0.01 Da for MS^1 and 0.025 Da for MS^2. For retention time, the range of 0.2-3.8 min was defined. For peak detection, an amplitude of 20000 was selected as the minimum peak height with a mass slice width of 0.05 Da. For deconvolution with the MS^2Dec algorithm, 1000 was set as the MS/MS abundance cut-off and 0.5 as the sigma window value. The ion species $[M-H]^-$ and $[M-H_2O-H]^-$ were defined. For peak alignment, the last fraction (fraction 120) was selected as the reference with a retention time (t_R) tolerance of 0.2 min and MS^1 tolerance of 0.02 Da. Removal of features based on blank filtering was selected. The results of the MS-DIAL processing were exported by generating an MS/MS spectral summary file (.MGF) and feature quantification table (.txt). The results were also imported to the MS-FINDER software[30] to determine the formula (mass tolerance ± 3 ppm) for each detected feature. The feature was excluded from the files when *a*) there was no match with any $C_xH_yO_z$ formula, *b*) the DBE value corresponding to the formula was less than 4, *c*) the feature was likely a fragment as it had a similar chromatogram with a higher *m/z* value (indicated by MS-DIAL), or *d*) the feature was also detected in consecutive fraction(s) at the same retention time. In the last case, only the feature with the most intensive signal (representing the maxima of the peak) was kept. Here, this procedure was done manually; however, automatic "demodulation" processes are under development to convert 2D data into 1D data that can be analysed with various novel softwares.[31] In addition, intensive background signals that were present in almost all MS^2 spectra (*m/z* 146.96, 188.94, and 119.95) were removed from the MS-DIAL output files. The edited output files were combined into one MGF and one .txt file containing all possible lignin features. Both files were used to construct the Feature-Based Molecular Network (FBMN) on the GNPS (gnps.ucsd.edu) platform.[32]

Because of the size of the combined files, they were first uploaded to the MassIVE repository (massive.ucsd.edu), after which they could be imported into the FBMN workflow on GNPS. MS-DIAL was selected as the Quantification Table Source and 0.02 Da was set as the mass tolerance for both precursor and fragment ions. The following values were selected as the network parameters: 0.6 as the minimum cosine score for a pair of consensus MS^2 spectra, 4 as the minimum number of shared fragment ions, 10 as the maximum number of nodes for one single node, and 0 as the maximum connected component size, which allows the connection of unlimited number of nodes in a single network. The default values were kept for the other input values. After running the FBMN workflow, the output network files were downloaded from the GNPS platform and imported to the Cytoscape software (version 3.9.1.) for visual editing.

For the structural characterisation of the detected features, the combined MGF file was imported and analysed in the SIRIUS software (version 5.6.3).[33,34] By using this software, it is possible to propose the molecular formula (SIRIUS) of a feature and elucidate its structure based on the fragmentation data (CSI:FingerID[35]). In the software, the MS^2 mass accuracy was set to 10 ppm, $[M-H]^-$ adduct was selected, and C, H, and O elements were allowed for the search of the molecular formula. The same $[M-H]^-$ adduct was selected for the fingerprint prediction and all the databases present in the software were applied for database search. In addition, the CANOPUS[36–38] function in the same software was applied to predict the compound class.

2.4.4 Peak capacity and coverage of the 2D separation space

Some figures of merit were calculated to characterise the performance of the 2D LC method for the analysis of this kind of depolymerised lignin sample. The most widely demonstrated values are peak capacity and orthogonality, which have proven to be suitable for the comparison of different 2D separation methods. However, as different methods can be used for the calculation of the values, we will briefly present the approaches used in this study.

The peak capacity (n_C) for a gradient separation can be individually estimated for both dimensions using the corresponding gradient time (t_g) and average peak width as 4σ (w) in time units according to Eq. 1:

$$n_C = \frac{t_g}{w} \tag{1}$$

However, for 2D separations, it is necessary to include the under-sampling correction factor (β) to take into account the peak broadening caused by the under-sampling during the ^{1}D (in the formula noted as D_1) fraction collection, which can be done by Eq. 2 presented in the work by Li *et al.*[39]:

$$n_{C,corrected}^{D1} = \frac{n_C^{D1}}{\beta} = \frac{n_C^{D1}}{\sqrt{1+3.35\times(\frac{t_s}{w^1})^2}} \tag{2}$$

where t_s is the sampling time. Under ideal conditions, the peak capacity of a 2D method can be calculated according to Eq. 3:

$$n_{C,theoretical}^{2D} = n_C^{D1} \times n_C^{D2} \tag{3}$$

When combining Eq. 1, 2, and 3, the equation for effective 2D peak capacity can be obtained, which is a more realistic value, as it also takes into account the effect of under-sampling.

$$n_{C,effective}^{2D} = \frac{n_C^{D1}\times n_C^{D2}}{\sqrt{1+3.35\times(\frac{t_s\times n_C^{D1}}{t_g^1})^2}} \tag{4}$$

The orthogonality was estimated using the convex hull approach.[40]

3. Results and discussion

3.1 Screening of columns for the ^{2}D SFC dimension

The selection of the suitable column for the ^{2}D SFC dimension was made based on the analysis of 33 monomer standards, which were selected to represent possible lignin monomers. Four columns were screened using generic gradient elution (5% – 50% of MeOH, normalised gradient slope of 3%, the other parameters can be seen in Table S2). With the Cortecs HILIC column, the majority of the standards co-eluted at dead time. In contrast, the Torus DEA column had very strong retention for some analytes

(pyrogallol; 3,4-dihyroxyphenylacetic acid; caffeic acid), causing peak broadening and difficulties with the detection of these compounds on the chromatogram. The strong retention of phenolic acids was also noted by Prothmann *et al.*[41] with Torus DEA and Torus 2-picolylamine columns. DIOL and 1-AA both exhibited a good separation over a similar elution range with a ΔC_e (difference of mobile phase composition at the elution of the most and least retained compounds) value of 22.3% for DIOL and 24.7% for 1-AA using the 33 monomer standards (Figure S1 in the SI). However, the 1-AA column has demonstrated a better separation of lignin monomers from dimers due to the enhanced selectivity provided by the π-π interactions between the double bonds of lignin compounds and the aromatic anthracene stationary phase.[42] As we expected that the depolymerised lignin sample involved in our study contains other compounds besides monomers, we selected the 1-AA column to investigate if this mechanism also aids the separation of higher oligomers in the 2D setup.

3.2 General characterisation of the off-line LC×SFC separation

To find the suitable elution ranges for the two dimensions, the depolymerised lignin sample was separately analysed with RPLC and SFC. The gradient times, flow rates, and other relevant factors for both dimensions were selected based on calculations that are presented in our previous study on the optimisation of an off-line LC×SFC method.[25] However, in the present work, we were able to collect 120 fractions instead of 80, which is beneficial for obtaining a higher effective peak capacity for the 2D method. Indeed, using Eq. 4, a very high effective peak capacity value – 3218 – was calculated for the LC×SFC method, demonstrating the high separation efficiency of the developed 2D method for the analysis of depolymerised lignin.

Figure 2 presents the obtained LC×SFC-HRMS plot using the BPC signal. Based on the convex hull approach, we calculated the coverage of the separation space to be 62%. Considering that the sample consists largely of neutral compounds with similar structures, the obtained value can be considered good. When taking into account the partial occupation of the separation space, the corrected peak capacity for the 2D method is 1995, which nowadays is still an unreachable value with 1D separations. In addition, as can be seen in Figure 2, there is no clustering of peaks on the upward or downward diagonals, demonstrating the low correlation and suitability of the selected dimensions for the analysis of neutral compounds present in depolymerised lignin.

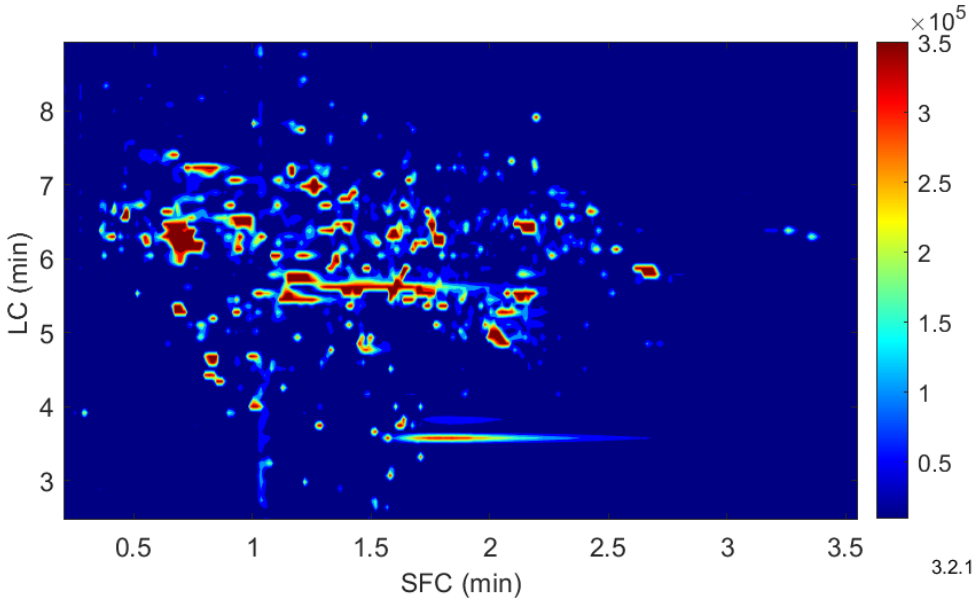

Figure 2. LC×SFC-HRMS BPC contour plot (MS^1) of depolymerised lignin.

3.3 MS-DIAL for the off-line LC×SFC-HRMS/MS data analysis

Depending on the data and research question at hand, different data analysis methods can be helpful in interpreting the measured tandem mass spectra. For the data obtained with the technique used in this study, an example is presented in Figure 3, showing the 2D plot for deprotonated $C_{16}H_{18}O_4$ and exemplary MS^1 and MS^2 spectra for two separated peaks. It can be seen that these two compounds are isomers with different fragmentation patterns and as the MS^1 and MS^2 spectra are clean of interfering signals and the MS^1 contains mainly just the pseudo-molecular ion, it was decided to apply mass-spectral software for the data analysis. The main advantage of using MS analysis software is the increased speed of the data analysis, which is especially beneficial in this study as the 2D analysis generated 120 data files. In addition, it can yield MS/MS data analysable with other approaches (here SIRIUS and FBMN). In this study, MS-DIAL software was first applied, which detects features and associated fragments by fitting the chromatograms of product ions to a precursor by using retention time.[16]

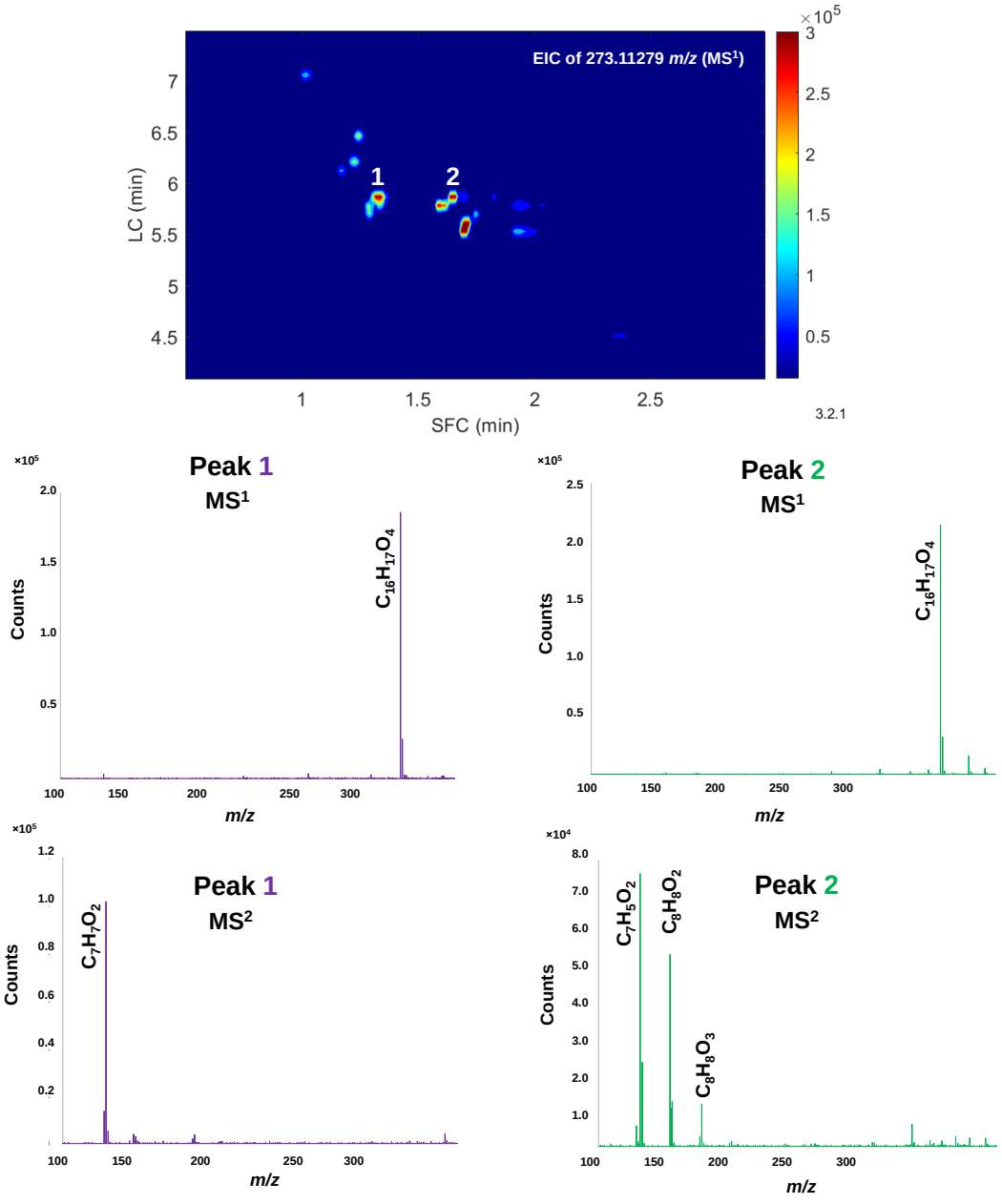

Figure 3. Example of mass spectra measured with the LC×SFC-HRMS method. In the first row is the LC×SFC-HRMS EIC contour plot (MS^1) of 273.11279 (± 5 ppm) *m/z*, which corresponds to the exact mass of deprotonated $C_{16}H_{18}O_4$. In the second and third row are the spectra that represent exemplary MS^1 and MS^2 spectra corresponding to the two separated isomers (Peak 1 and Peak 2), respectively.

In addition to true features originating from the compounds of the sample, MS-DIAL can also pick up so-called false features. These can be signal noise, system contamination, or in-source fragmentation.[43] Even with ESI, which is considered to be the softest ionisation technique, some compounds can have in-source fragmentation.[44] Therefore, when there are many analytes eluting simultaneously, it becomes more and more difficult to distinguish true features from fragments (false features), especially when the analytes are very similar. In this study, we manually checked features for which the MS-DIAL software showed an alert "Chromatogram similar" and removed the features with lower *m/z* values. Those features are likely in-source fragments, because their peak shapes were similar to the peak shape of the molecular ion and the *m/z* value corresponded mainly to the loss of CH_3 or CO.

MS-DIAL has been shown to enable the deconvolution of DIA MS/MS spectra for compounds that co-elute to some extent.[45] However, the precursors have to have different exact masses and for an efficient deconvolution, there has to be at least two data-point difference between the maxima of the chromatographic peaks.[46] Recent advancements such as CorrDec[46] (which has been added to MS-DIAL version 3.22 and up) have been shown to enable the deconvolution of even completely co-eluting compounds. However, this approach requires that the analysis of the sample would be repeated at least ten times, which would make the off-line 2D LC analysis of one sample dreadfully long. Also, for the time being, there is no evidence that it would be able to deconvolute isomers, which signifies that powerful chromatographic separation is still needed before the MS detection.

3.4 Classification of the detected lignin compounds

All of the 120 data files (in .ABF format) obtained from the LC×SFC-HRMS/MS measurement were loaded to MS-DIAL and analysed with the parameters described in section 2.4. After combining the results, 471 pseudo-molecular ions corresponding to a $C_xH_yO_z$ formula with DBE $\geq$ 4 were detected in the depolymerised lignin sample (Table S3 in the SI). DBE (Double Bond Equivalent, also Ring Double Bond Equivalent aka RDBE or RDB is sometimes used for the naming) is a value that can be used to classify detected compounds, including lignin depolymerisation products. Depending on the experimental conditions of the depolymerisation and on other additional sample pre-treatment processes, such as fractionation, the lignin sample can contain monomers (analytes with one aromatic core), dimers (two aromatic cores), trimers (three aromatic cores), and so on. Looking at the structure of lignin in Figure 1, the DBE value for monomers should generally stay in the range of 4-7, for dimers in the range of 8-11, for trimers 12-15, and so forth. As the MS-DIAL software yielded exact masses for all of the features, it was possible to find the molecular formula and, from that, the DBE value. For the analysed sample, the three most retained compounds in the SFC dimension also had the highest DBE value (17, generally corresponding to tetramers). After those compounds, there was no UV signal, confirming that the sample did not contain oligomers higher than tetramers.

Based on the DBE value, the detected features were plotted on an LC×SFC plot (Figure 4) with the same retention times as was seen in Figure 2. As hypothesised, the detected features are clustered together based on their DBE value corresponding possibly to a mono-, di-, tri-, or tetramer. This phenomenon can again be explained by the π-π interactions between the depolymerised lignin aromatic ring(s) and the anthracene moiety of the 1-AA stationary phase. This kind of classification can be used to detect outliers for further investigation. In Figure 4, the compounds that are likely not lignin compounds are marked with crossed-out squares, as their structural candidates and compound classes in SIRIUS were

far from potential lignin compounds (e.g., aliphatic compounds, terpenoids). This classification can also help with comparing samples to each other without the need for a detailed structural study. This kind of visual comparison based on grouping on 2D plots is a very common approach in 2D GC but much less explored in 2D LC.[4]

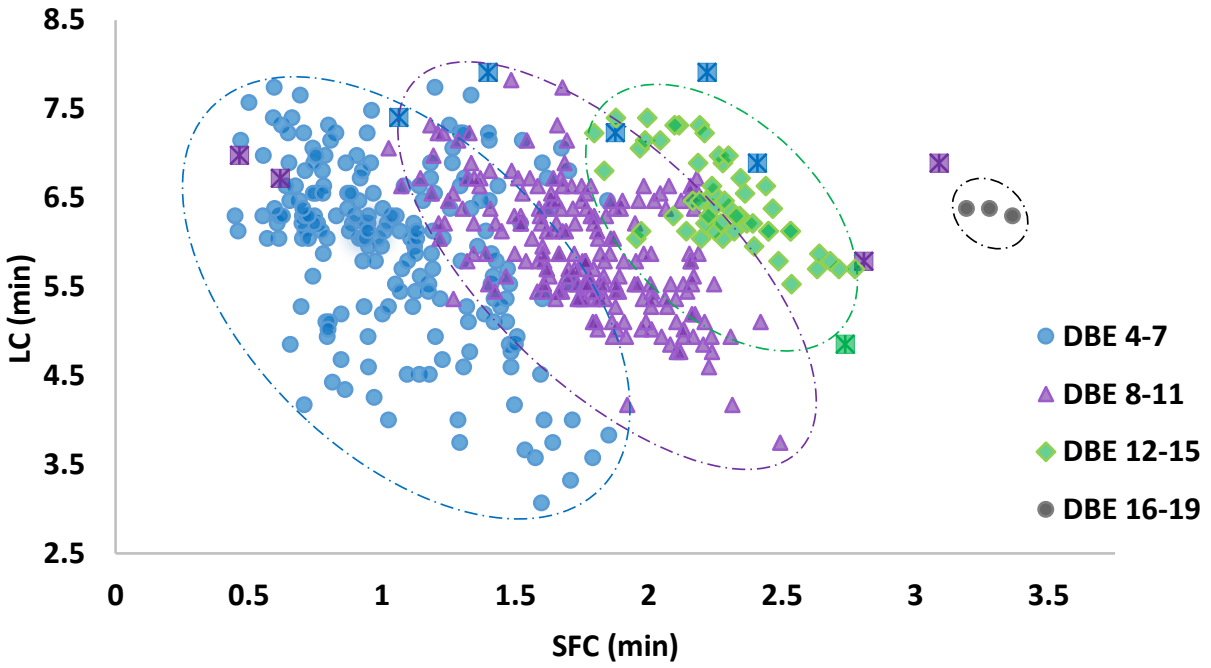

Figure 4. LC×SFC-HRMS plot (MS^1) of $C_xH_yO_z$ compounds (DBE ≥ 4) detected with MS-DIAL in the depolymerised lignin sample. The same data that was used in Figure 2 is also presented here. The ovals with dashed lines represent the clusters of lignin compounds with DBE 4-7 (blue dots, likely monomers), 8-11 (purple triangles, likely dimers), 12-15 (green diamonds, likely trimers), and 16-19 (black dots, likely tetramers). The outliers that are presumably not lignin compounds are presented with crossed-out squares.

At the same time, one must be careful, as there can also be lignin compounds that have a DBE value corresponding to a higher class of the presented DBE ranges. For example, as was shown in the SI of a publication by Prothmann *et al*.[5], additional double bonds in the structure of a dimer can yield a DBE value that classically corresponds to a trimer. Therefore, for the sample analysed in our work, we studied the potential structural candidates proposed by the SIRIUS software based on the comparison of MS/MS pattern to see if the candidates belong to the class implied by the DBE value or not (Table S4 in the SI). This was merely done to see if the candidates matched mainly mono-, di-, tri-, or tetramers, not to tentatively identify all the structures of the detected compounds, as this is not the aim of this work. In the case of compounds with a DBE value of 4-7, 185 compounds had one aromatic ring, 9 corresponded more to unsaturated aliphatic compounds, and 3 had candidates matching to a similar extent to compounds both having and not having an aromatic ring. With DBE value of 8-11, there were 202 compounds whose candidates all matched dimers and 1 that matched with monomers. With DBE range 12-15, 24 compounds matched largely trimers, 8 had candidates mostly corresponding to dimers, and 13 had both dimers and trimers as equally potential matches. For DBE 16-19, 1 compound matched tetramers and 1 compound could be either trimer or tetramer. Therefore, under the classical DBE ranges, 94% had indeed highest matches with monomers, almost 100% with dimers, 53% with trimers, and one out of two to tetramers. This suggests that some of the compounds classified by the DBE value could be indeed smaller by one aromatic ring. To determine how much misclassification using DBE value can cause, it would be necessary to analyse oligomer standards (which are scarce, as mentioned before) or have a good match in the SIRIUS software.

The SIRIUS software uses structural fingerprints that have been predicted from the structures of potential candidates found in chemical databases. For this, the corresponding structure has to be present in one of the databases (such as PubChem, COCONUT) utilised by the software. In the case of the detected compounds, over 95% had the first match with a compound that was present also in the PubChem database. Therefore, to get an idea how well the PubChem database covers lignin compounds, we searched for the lignin oligomers tentatively identified in the study by Prothmann *et al*.[5] As can be seen in Table S5 in the SI, out of the 35 compounds, only one had an exact stereo isotope match in PubChem. For 12 compounds, there were no isomers matching at least with 90% of structural similarity. These included all those dimers that had a DBE value classically corresponding to trimers. This demonstrates, that the databases contain only a small part of the potential structures, as lignin oligomers with all of the potential structures caused by the isolation and depolymerisation are quite understudied compounds. However, some oligomers had up to 69 isomers present in the PubChem database, which allows for some compounds to have a match at least with a structurally similar structure. In addition, for a lot of the potential tri- and tetramers and for some dimers detected in our study, the match factor in SIRIUS was quite low (around 50% or less). Therefore, for more reliable structural characterisation of lignin compounds, specific lignin databases, further fragmentation studies, or manual elucidation of the MS/MS spectra would be necessary. However, applying the SIRIUS software still enabled us to demonstrate the benefits of using the 2D chromatographic method for the analysis of lignin before MS/MS, which was the aim of our study. In addition, the classification based on DBE value can still help to determine the possible class of monomer/oligomer, detect outliers for further investigation, and compare samples at large.

3.5 Investigation of the separation mechanism

Although the analysis of the depolymerised lignin sample demonstrated the classification of lignin compounds based on their DBE values on the 2D plot (Fig. 4), the analysis of monomeric standards aids to study the separation mechanisms more in-depth. Therefore, the same 33 monomer standards that were used for column screening were analysed with the optimised LC and SFC methods. In Figure 5, the placements of the monomer standards on the 2D LC×SFC-HRMS plot are presented (the names of compounds are shown in section 2.1 and Table S1). By studying the retention of similar standards 31 and 33, it can be seen that an additional double bond in the structure increases the retention in the SFC dimension. Comparison of the retention of standards 4 and 8, which differ only in the position of the double bond, demonstrates that a higher number of conjugated double bonds increases retention with the 1-AA column. Once again, this is caused by the π-π interactions, which are stronger in the case of larger conjugated structures.[47]

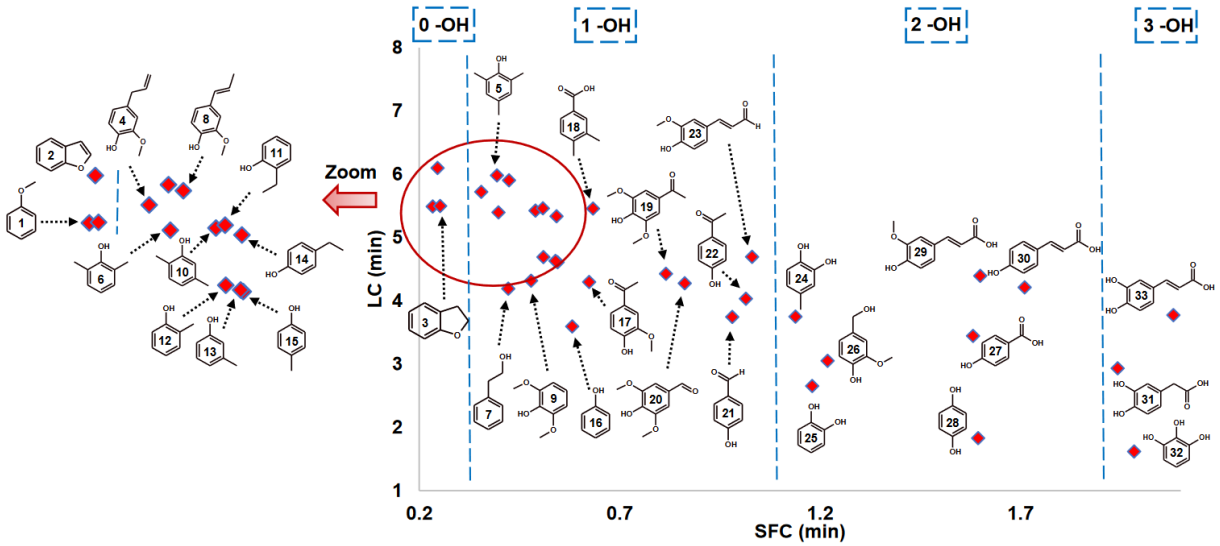

Figure 5. 2D LC×SFC-HRMS plot of the monomer standards. The plot was constructed by combining the 1D LC and 1D SFC retention times of the standards. The names of the compounds corresponding to the numbering are shown in section 2.1 and Table S1. Dashed blue lines separate roughly the sections based on the number of hydroxyl groups in the monomer structure.

Another mechanism that plays a major role in the separation is the hydrogen bonding interaction. As can be seen by the vertical dashed blue lines in Figure 5, in the case of the analysed standards, the SFC dimension can be roughly sectioned based on the number of hydroxyl groups in the structure of the monomers. The more hydroxyl groups are in the structure of the compound, the stronger the hydrogen bonding interaction with the 1-AA polar sites, which in turn leads to increased retention. For example, standard 32 (3 –OH) has a higher retention time than 25 (2 –OH), but 25 has higher retention than 16 (1 –OH). The same behaviour can also be seen for more complex monomers, such as 29 (2 –OH) and 23 (1 –OH). However, this polar interaction can be sterically hindered by other functional groups present in the structure of the compound. For example, standard 6 eluted earlier in the SFC dimension than its positional isomer 10 because, in the structure of 6, both methyl groups are next to the hydroxyl group, weakening the polar interaction. Retention of standards 25 and 28 demonstrates the same effect even for compounds that have just –OH functional groups. The steric effect on SFC retention behaviour can also be observed for non-isomeric standards, such as 9 and 16, 29 and 30. Although we presume that the same interactions affect the separation of oligomers, without standards, we cannot propose a sectioning for oligomers.

The utilisation of the RPLC dimension in ^{1}D enables additional separation based on hydrophobicity. This can be seen, for example, when studying the log*P* (octanol-water partition coefficient) values and retention of standard 14 compared to 13 and 15 in the direction of the LC axis. Based on the publication by Smith *et al.*[48], for standard 14, a log*P* value of 2.50 has been found, which is in correspondence with the higher retention in LC compared to standards 13 and 15, with both having a log*P* value of 1.97. Moreover, the F5 (pentafluorophenyl propyl) phase is known for its combination of hydrophobic, aromatic, and steric separation mechanisms which also contributed to the improved selectivity of isomeric species such as monomers 4 and 8. Therefore, the developed 2D LC×SFC method enables the separation of compounds based on hydrophobicity, the number of hydroxyl groups, steric effects, position and number of double bonds. Having this kind of various interactions can be especially beneficial for the (improved) separation of positional isomers.

3.6 Elucidation of the detected compounds in the depolymerised lignin sample

The most straightforward way to determine whether a compound is present in the depolymerised lignin sample is to use reference standards, such as the same 33 standard compounds selected based on previous studies. Thanks to the multi-dimensional LC×SFC-HRMS/MS method, the elucidation of compounds can be made based on four criteria – retention times in RPLC and SFC, accurate mass, and fragmentation pattern. As has been proposed by Schymanski *et al.*[49], this yields a confidence level of 1, and as the authors say, the application of an orthogonal method (as we have done here by applying both LC and SFC) confirms this confidence level. For determining the t_R reproducibility of the SFC dimension, Mix A containing monomer standards nr 4, 5, 11, 16, 20, and 28 was analysed during three days, each with a repetition of five. Using the EIC signal of each molecular ion, a within-lab reproducibility value of 0.012 min was calculated (3-fold the mean of t_R standard deviations). Because of the fraction collection, one sampling time was selected as the reproducibility of the ^{1}D RPLC dimension. Therefore, the following criteria were applied: *a*) t_R in RPLC (± 0.085 min); *b*) t_R in SFC (± 0.012 min); *c*) accurate mass of precursor (± 3 ppm); and *d*) MS^2 match over 90% in SIRIUS. Interestingly, only two of the 33 standards (19: acetosyringone and 22: 4-hydroxyacetophenone) were identified within the lignin sample, matching all criteria (overlay can be seen in Figure 6). No other standard matched even the first three criteria. This demonstrates that because of the complexity of a natural depolymerised sample, it is very difficult to obtain corresponding standards for identification without performing some preliminary structural characterisation.

In the interest of obtaining more information about the detected compounds in the depolymerised lignin sample, SIRIUS software was used. In addition to the software provided match scores with potential candidates, knowing also the retention mechanisms in the two dimensions aids to give additional assessment for the proposed candidates. As hydrophobicity is the driving force for separation in the RPLC dimension, the log*P* value of the candidate has to be reasonable in relation to the t_R. In the SFC dimension, when using the 1-AA stationary phase, the number and position of hydroxyl groups have an effect on the retention, which can aid with the structural characterisation of similar, or even isomeric, compounds. Overall, these aspects can help evaluate the suggested candidates and propose some tentative structures. Therefore, in Figure 6, the tentative structures for some of the monomers and dimers detected in the depolymerised lignin sample are proposed.

In the case of monomeric compounds, it was easier to find correlations and exclude illogical candidates because of their simpler structure. A similar rough sectioning based on the number of hydroxyl groups that was seen with standards was also seen with the monomeric compounds (black dashed lines in Figure 6). As there are no compounds in the area of none or three –OH groups, we can presume that all monomers had at least one or two hydroxyl group(s). Compared to the monomeric standards, the monomers in the real-life sample (blue dots in Figure 6) had generally higher retention in the RPLC dimension, which suggests that those compounds are more hydrophobic. These two observations were confirmed by studying their possible structures with the SIRIUS software. For example, as seen in Figure 6, the possible structures of compounds A, B, F, and I all have more nonpolar side chains that lead to higher hydrophobicity, which in turn leads to higher retention in RPLC. This can aid with the separation of isomers, as can be seen with compound G, which has the same formula as standard 23 ($C_{10}H_{10}O_3$). These compounds showed similar retention in SFC but good separation in RPLC. In the SFC dimension, isomers K and O had highly similar fragmentation patterns, leading to the suggestion of the same around 10 positional isomers for both compounds with a SIRIUS match factor over 80%. However, studying the position on the 2D plot suggests that these compounds have similar log*P* values but different hindrances of the –OH groups. Using these characteristics, we propose tentative structures for the two compounds, where the –OH groups are more hindered in compound K and less in compound O. In terms of log*P* value, for the presented compounds only N has a very low value. This again suggest that the real structure of the detected compound is absent from the used databases.

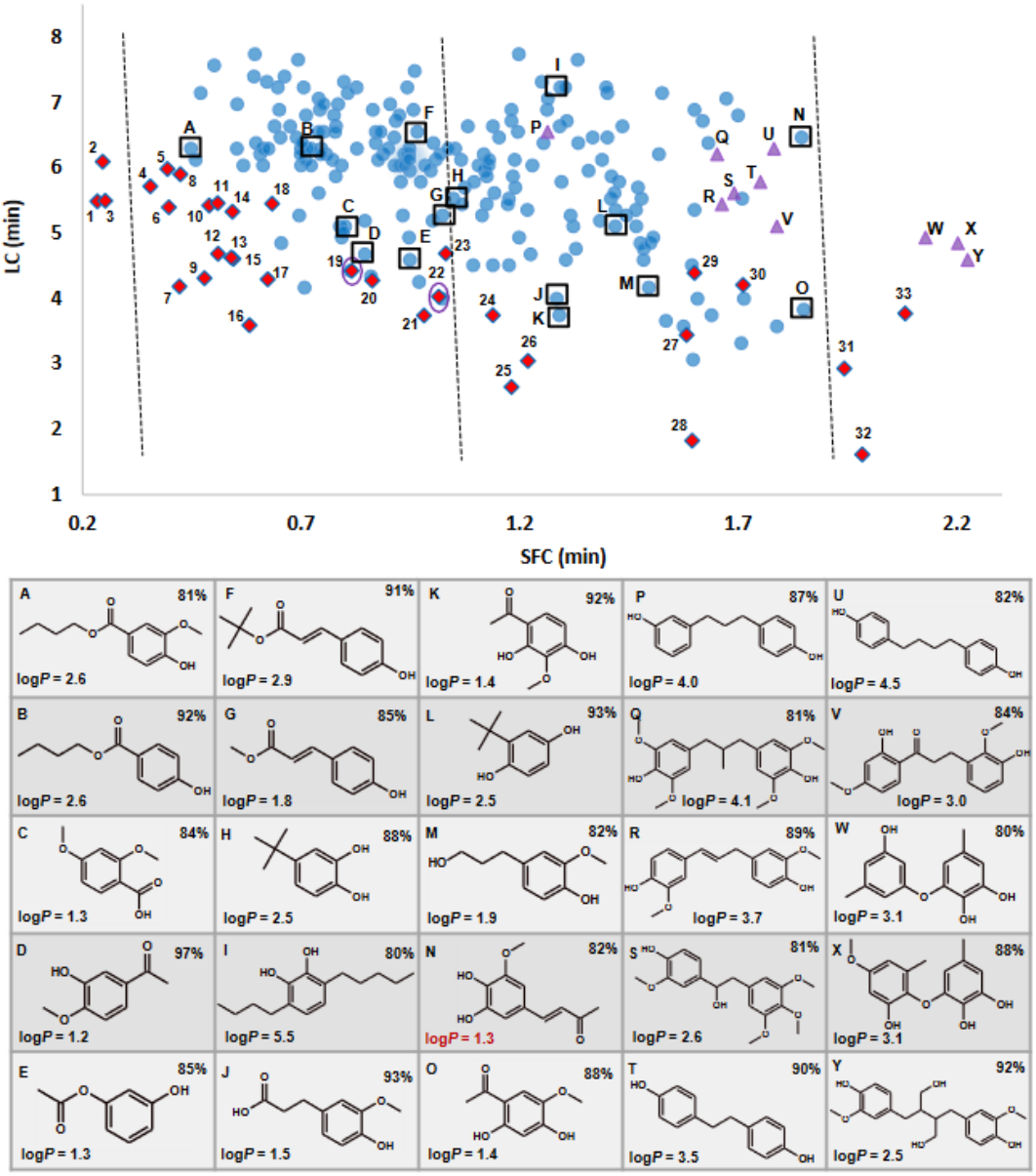

Figure 6. LC×SFC-HRMS plot of monomer standards (red diamonds with numbers) and some of the compounds detected in the depolymerised lignin sample: all compounds having DBE 4-7 (blue dots) and some of the compounds having DBE 8-11 (purple triangles). For monomer standards, the retention data was obtained from 1D LC and 1D SFC analyses and combined into a 2D plot. For the selected lignin compounds, the retention times are the same as in Figures 2 and 4. The dashed black lines indicate the rough sectioning for monomeric compounds based on the number of hydroxyl groups. The monomers that could be identified in the real-world sample by using corresponding standards are highlighted with purple ovals. Black rectangles and letters A to Y highlight some unknowns for which we propose one of the possible structures that had a SIRIUS match over 80%, reasonable computed log*P* value and number/position of hydroxyl groups. The log*P* values were obtained from the SIRIUS software and correspond to the XLog*P* values calculated using the Chemical Development Kit CDK. The letters of the compounds correspond to the following ID numbers shown in Table S3: A – ID 279; B – ID 256; C – ID 60; D – ID 30; E – ID 25; F – ID 345; G – ID 77; H – ID 117; I – ID 437; J – ID 11; K – ID 6; L – ID 59; M – ID 14; N – ID 324; O – ID 9; P – ID 346; Q – ID 270; R – ID 108; S – ID 148; T – ID 166; U – ID 280; V – ID 66; W – ID 47; X – ID 39; Y – ID 28.

For dimers and higher oligomers, the interpretation of elution order is more complex as there is an interplay of the interaction factors, none of which is largely dominating. As those compounds have more aromatic rings than monomers, the elution in the SFC dimension is shifted to higher retention times (as can be seen by the classifications in Figure 4). The higher number of double bonds also leads to a higher

probability of having longer conjugated systems in addition to less straightforwardly interpretable steric effects, meaning that the –OH zones were not as clear. The absence of oligomer structures from databases also amplifies the complexity. However, the same ordering of compounds based on interaction mechanisms that were seen for monomeric compounds was also seen for some of the possible dimers. Figure 6 shows some examples of tentative dimer structural elucidation. Compound U had higher retention in the RPLC dimension than compound T, presumably because of the longer alkane chain. Compound P is a similar compound to T and U, but because of the lower retention in the SFC dimension, we presume that the positions of the two –OH groups have to be located so that there are more steric effects impeding the polar interactions. In the structure of compound P, probably the positions of the –OH groups are located so that there is even more hindrance; however, for this compound, there were only a few isomers available in the databases used by the SIRIUS software.

The structures of the tentatively annotated monomers and dimers have quite unusual structures containing saturated side chains and linkages. However, the sample analysed in this work was obtained from the partial depolymerisation of lignin that was performed under hydrogen atmosphere, which can cause reduction of double bonds. Of course, to confirm these conclusions about the structures of potential dimers, again standards or databases including more lignin compounds would be needed.

Overall, involving an annotation software in the data analysis helped to elucidate the structures of unknown compounds, which in turn demonstrated the usefulness of the 2D chromatographic separation method for the non-target analysis of complex mixtures. Besides powerful separation, the combined LC×SFC-HRMS/MS method also helps to reduce the number of candidates for each feature by incorporating the logic of the retention mechanisms.

3.7 Comparison of the 2D LC×SFC method to 1D SFC

The developed LC×SFC method was compared to a long (gradient time 30 min) 1D SFC separation of the same depolymerised lignin sample. For the 1D method, SFC was selected instead of RPLC to have the same ionisation conditions as the 2D method, thus ensuring a fair comparison independent of ionisation (in some cases, SFC has contributed to an improved ionisation).[12] As discussed before, the corrected peak capacity of the LC×SFC method was 1995. For the 1D SFC separation of the depolymerised lignin sample, a much lower value – 155 – was found for the peak capacity. Therefore, by using the 2D setup, more than 12-fold higher peak capacity could be obtained for this sample.

3.7.1 Separation of isomers

In addition to miss-annotations caused by unwanted in-source fragmentation, the poor chromatographic separation of isomers can also lead to false annotations.[44] Besides observing a decrease in co-elutions for compounds with different accurate masses, isomers also had better separation in 2D. This can be especially beneficial for the analysis of depolymerised lignin, as out of the detected $C_xH_yO_z$ compounds with DBE $\geq$ 4, almost 77% had at least one isomer (361 features out of 471) detected in the same sample (Table S3 in the SI). For example, for deprotonated $C_{18}H_{20}O_5$, there were even 12 isomers detected in the sample. In terms of discriminating isomers, one of the following criteria has to be fulfilled. The straightforward case is when the retention times of the isomers are sufficiently different, thus giving MS^2 spectra corresponding only to one of the compounds.[18] However, when the isomers co-elute, the MS^2 spectra will have a mixture of product ions originating from two compounds. In that case, researchers have demonstrated that the co-eluting compounds can be differentiated when *i*) they have characteristic fragmentation or *ii*) corresponding standards can be used to elucidate their mass spectrometric fragmentation pathways.[50–53] If one of these criteria is not met, then not even highly powerful data analysis tools can currently aid with the deconvolution.[51] In the case of target analysis with standards, it is possible to use on-line LC×LC with heart-cutting mode allowing the known co-

elutions in ^{1}D to be separated with a shallower gradient in the ^{2}D.[53] However, multiple heart-cutting mode is technically limited in on-line configuration and so the detection of co-eluting isomers is especially complex in the case of non-target analysis as it is impossible to detect (or even know) co-elution of isomers when there is no evidence to suspect their presence in the 1D separation. Comprehensive 2D chromatography analysis involving a second dimension with high isomer resolution requires a shallow ^{2}D gradient that so far only off-line configuration can provide.

Although, in some cases, SFC has shown to have a more efficient separation of isomers than RPLC,[54] in our study, we found that both LC and SFC dimensions are necessary for the analysis of depolymerised lignin. For example, in Figure 7, when extracting the *m/z* value of 341.10263, only two major peaks are seen on the 1D chromatogram, whereas the LC×SFC plot has four major peaks. As can be seen by looking at the parallel lines on the EIC of the 2D plot in Figure 7, in the case of 1D analysis, there would be co-elution of these isomers, regardless of whether RPLC or SFC would be used. Using MS-DIAL for the 1D-SFC data also detected the same two peaks as two spots because the software spots precursor ions peaks by monitoring two continuous data axes: retention time (t_R) and accurate mass (*m/z*).[16] However, applying the developed 2D LC×SFC method, it was possible to detect six isomers for this formula. This included a compound with a much lower intensity (ID 49) compared to its isomers that would have co-elution when only the SFC dimension would be used (ID 313 and 132). Therefore, using the 2D separation method yields MS data that corresponds to the separated isomer (and not a combination of ions from the co-elution) and also enables the detection of much less intense isomers.

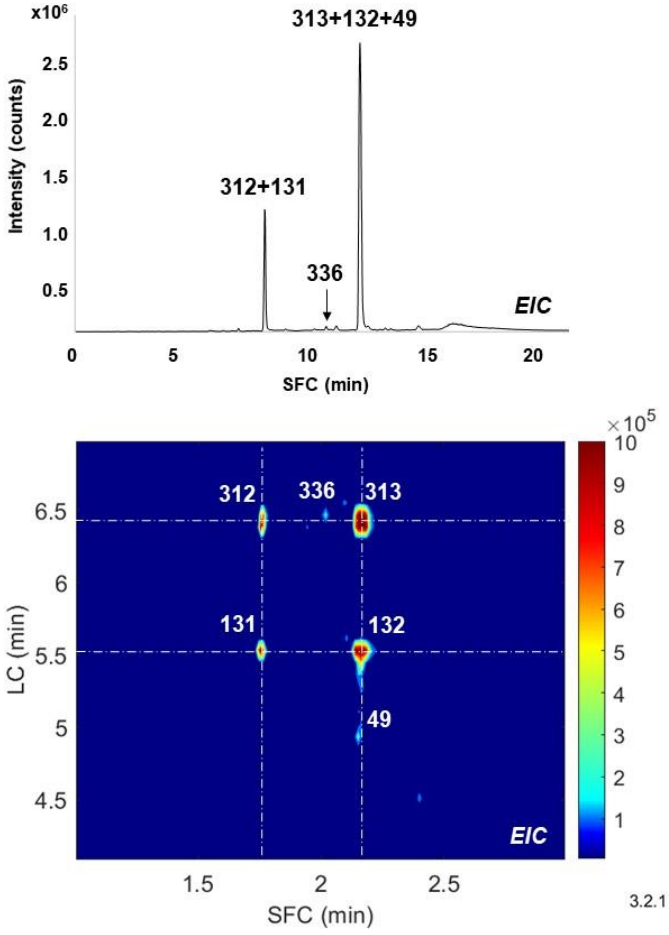

Figure 7. Comparison of 1D SFC-HRMS (top row) to 2D LC×SFC-HRMS (bottom row) based on the separation of isomers. A value of 341.10263 *m/z* (± 5 ppm) was used to construct the EICs, which corresponds to deprotonated $C_{19}H_{18}O_6$ and DBE of 11. The ID numbers of detected isomers (312, 131, 336, 313, 132, and 49) correspond to the numbering presented in Table S3 in the SI. The BPC of the 1D SFC analysis is shown in Figure S2 in the SI.

3.8 FBMN – Feature-Based Molecular Network

As the final step, Molecular Network (MN) was applied. MN connects together features that have similar fragmentation; thus, we can obtain more information about their structural similarities. For LC×SFC data, MN has been used by Wei *et al.*[24], where precursor ions within a defined mass tolerance range and nearly identical MS^2 spectra were merged into a single node. This was beneficial for the removal of features that are caused by the collection of the same analyte into consecutive fractions. However, MN would also fuse together those isomers with similar MS^2 that have *i*) different retention time in ^2D or *ii*) the same retention time in ^2D but baseline separation in ^1D (features in non-consecutive fractions). This issue can be overcome by using FBMN (a type of MN), which enables the visualisation of features with the same accurate mass by also including MS^1 information, such as t_R.[32] Such an approach can be especially beneficial for the analysis of depolymerised lignin, as the sample analysed in our study contained a very high number (approx. 77%) of isomers.

In Figure 8, the FBMN for the depolymerised lignin sample analysed with the 2D LC×SFC-HRMS/MS method is presented. With the applied generic GNPS parameters, 318 compounds out of the 471 were connected in the main network (shown in Figure 8), and the other compounds were in clusters where there were less than five nodes. In orange are highlighted all features corresponding to deprotonated $C_9H_{10}O_4$, which were noted with O (ID 9), K (ID 6), and C (ID 60) in Figure 6. It was seen that feature 9 is directly connected to feature 6 (red dashed line), which supports the proposition that these compounds are positional isomers, as was discussed in section 3.6. Although compound 60 (noted as C in Figure 6) also has the same formula as the previous two compounds, it is connected to feature 6 through another non-isomer feature. This is consistent with the structural candidates as feature 60 seems to have different side groups and is probably not a positional isomer to 9 and 6.

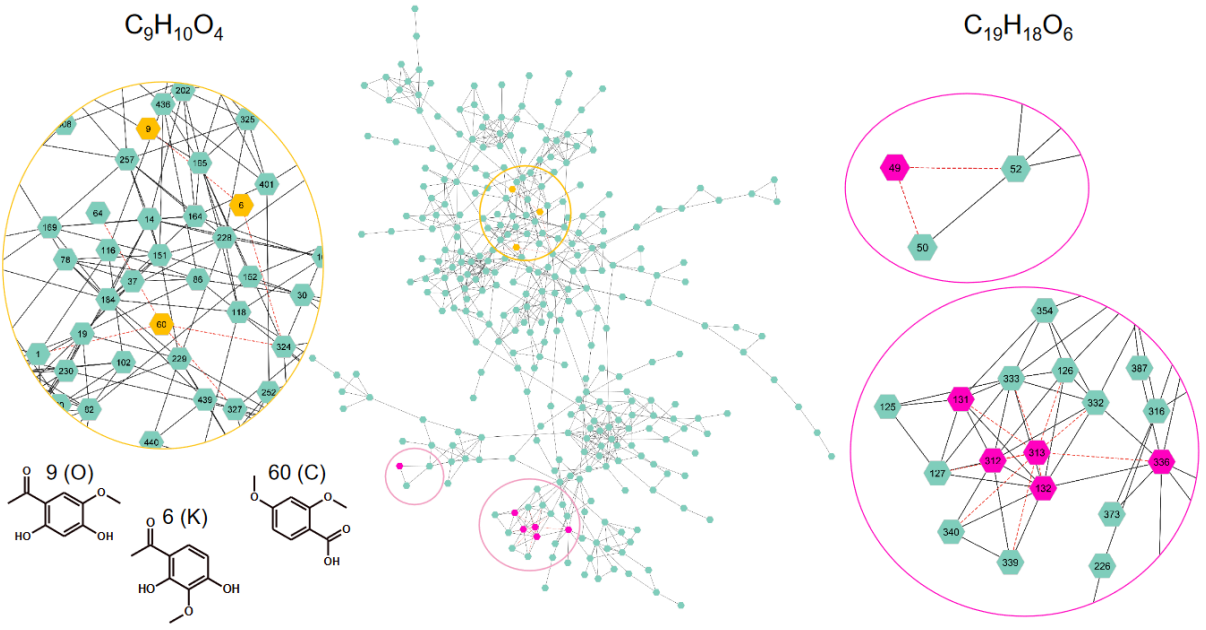

Figure 8. Feature-Based Molecular Network (FBMN) of the depolymerised lignin sample analysed with the LC×SFC-HRMS/MS technique, and visualised in Cytoscape. All the detected features corresponding to deprotonated $C_9H_{10}O_4$ and $C_{19}H_{18}O_6$ are shown in orange and pink, respectively. All the edges showing all connections for features with ID 9, 6, 60, 49, and 313 are highlighted with red dashed lines. For the compounds highlighted with orange, the tentative structural candidates are presented, where the number corresponds to the feature ID (Table S3 in SI) and the letter to the notation used in Figure 6.

Applying the same argumentation, we can also study the location of other isomers, for example, isomers corresponding to deprotonated $C_{19}H_{18}O_6$, which was also the example in Figure 7. In Figure 8, all isomers matching this formula are highlighted with pink colour. As can be seen with the red dashed lines, 313 is directly connected to four of the isomers, demonstrating that five out of six isomers have similar MS^2 patterns. This suggests that all except compound 49 are highly similar, possibly positional, isomers. Therefore, FBMN has demonstrated to rapidly define and visualise if the isomers are structurally highly similar (including positional isomers) or more different from each other.

4. Conclusions

In this work, a powerful comprehensive off-line 2D RPLC×SFC-HRMS/MS method was applied for the non-target analysis of depolymerised lignin. The method enabled the detection of 471 $C_xH_yO_z$ compounds with DBE ≥ 4, where the highest DBE value was 17 (classically corresponding to tetramers). In addition, the 2D plot showed a classification of the lignin compounds based on their DBE range largely corresponding to the number of aromatic rings in the structure. This kind of classification can be used to find outliers (as was demonstrated here) or to compare different samples to each other.

The analysis of 33 monomeric standards enabled to investigate the 2D separation mechanism in more detail. It was seen that the 2D LC×SFC separation was based on hydrophobicity, number of hydroxyl groups, steric effects, and position/number of double bonds in the structure of the analyte. Understanding the separation mechanism helped to characterise the LC×SFC-HRMS/MS results of the depolymerised lignin and evaluate the structural candidates proposed by the SIRIUS software. In addition, the 2D approach yielded clean MS^1 and MS^2 spectra that could be more easily analysed with mass spectral analysis softwares (in this study, MS-DIAL, SIRIUS, and FBMN). However, it was seen that there is a need for additional developments to improve the structural characterisation of lignin compounds with annotation softwares.

Compared to a long 1D SFC method, the 2D technique provided an improved separation of compounds, including isomers. In terms of lignin analysis, this is highly beneficial, as 77% of the detected features had at least one corresponding isomer detected in the same sample. The FBMN additionally helped to study the possible structural candidates of the isomers based on their MS^2 spectral similarities. The established strategy could also suit the (non-target) analysis of other isomer-rich mixtures with neutral compounds. Therefore, we have demonstrated that powerful chromatographic methods are needed (such as the one applied here) for a more reliable identification based on mass spectral data. In relation to isomers, this could be especially beneficial as the annotation of co-eluting isomers is still an unsolved challenge.

Acknowledgments

This work was funded by the French National Research Agency (project BIOPOLIOL, ANR-21-CE43-0026). The authors would like to thank Dr. Pilleriin Peets and Ph.D. candidate Helen Sepman for fruitful discussions about the data analysis involving MS-DIAL and SIRIUS softwares. The anonymous reviewers are also acknowledged for their constructive comments and help in improving the manuscript.

References

(1) Constant, S.; Wienk, H. L. J.; Frissen, A. E.; Peinder, P. de; Boelens, R.; Es, D. S. van; Grisel, R. J. H.; Weckhuysen, B. M.; Huijgen, W. J. J.; Gosselink, R. J. A.; Bruijnincx, P. C. A. New Insights into the Structure and Composition of Technical Lignins: A Comparative Characterisation Study. *Green Chem.* **2016**, *18* (9), 2651–2665. https://doi.org/10.1039/C5GC03043A.

(2) Sethupathy, S.; Murillo Morales, G.; Gao, L.; Wang, H.; Yang, B.; Jiang, J.; Sun, J.; Zhu, D. Lignin Valorization: Status, Challenges and Opportunities. *Bioresour. Technol.* **2022**, *347*, 126696. https://doi.org/10.1016/j.biortech.2022.126696.

(3) Bertella, S.; Luterbacher, J. S. Lignin Functionalization for the Production of Novel Materials. *Trends Chem.* **2020**, *2* (5), 440–453. https://doi.org/10.1016/j.trechm.2020.03.001.

(4) Tammekivi, E.; Geantet, C.; Lorentz, C.; Faure, K. Two-Dimensional Chromatography for the Analysis of Valorisable Biowaste: A Review. *Anal. Chim. Acta* **2023**, 341855. https://doi.org/10.1016/j.aca.2023.341855.

(5) Prothmann, J.; Spégel, P.; Sandahl, M.; Turner, C. Identification of Lignin Oligomers in Kraft Lignin Using Ultra-High-Performance Liquid Chromatography/High-Resolution Multiple-Stage Tandem Mass Spectrometry (UHPLC/HRMSn). *Anal. Bioanal. Chem.* **2018**, *410* (29), 7803–7814. https://doi.org/10.1007/s00216-018-1400-4.

(6) Sun, M.; Sandahl, M.; Turner, C. Comprehensive On-Line Two-Dimensional Liquid Chromatography × supercritical Fluid Chromatography with Trapping Column-Assisted Modulation for Depolymerised Lignin Analysis. *J. Chromatogr. A* **2018**, *1541*, 21–30. https://doi.org/10.1016/j.chroma.2018.02.008.

(7) Joffres, B.; Nguyen, M. T.; Laurenti, D.; Lorentz, C.; Souchon, V.; Charon, N.; Daudin, A.; Quignard, A.; Geantet, C. Lignin Hydroconversion on MoS2-Based Supported Catalyst: Comprehensive Analysis of Products and Reaction Scheme. *Appl. Catal. B Environ.* **2016**, *184*, 153–162. https://doi.org/10.1016/j.apcatb.2015.11.005.

(8) Abdelaziz, O. Y.; Brink, D. P.; Prothmann, J.; Ravi, K.; Sun, M.; García-Hidalgo, J.; Sandahl, M.; Hulteberg, C. P.; Turner, C.; Lidén, G.; Gorwa-Grauslund, M. F. Biological Valorization of Low Molecular Weight Lignin. *Biotechnol. Adv.* **2016**, *34* (8), 1318–1346. https://doi.org/10.1016/j.biotechadv.2016.10.001.

(9) Staš, M.; Auersvald, M.; Vozka, P. Two-Dimensional Gas Chromatography Characterization of Pyrolysis Bio-Oils: A Review. *Energy Fuels* **2021**, *35* (10), 8541–8557. https://doi.org/10.1021/acs.energyfuels.1c00553.

(10) Donato, P.; Cacciola, F.; Mondello, L.; Giuffrida, D.; Beccaria, M.; Dugo, P.; Domenica Mangraviti; Ivana Bonaccorsi; Margita Utczas. Analysis of the Carotenoid Composition and Stability in Various Overripe Fruits by Comprehensive Two-Dimensional Liquid Chromatography. *LCGC Eur.* **2016**, *29* (5), 252–257.

(11) Oliveira Lago, L.; Swit, P.; Moura da Silva, M.; Telles Biasoto Marques, A.; Welke, J.; Montero, L.; Herrero, M. Evolution of Anthocyanin Content during Grape Ripening and Characterization of the Phenolic Profile of the Resulting Wine by Comprehensive Two-Dimensional Liquid Chromatography. *J. Chromatogr. A* **2023**, *1704*, 464131. https://doi.org/10.1016/j.chroma.2023.464131.

(12) Burlet-Parendel, M.; Faure, K. Opportunities and Challenges of Liquid Chromatography Coupled to Supercritical Fluid Chromatography. *TrAC Trends Anal. Chem.* **2021**, *144*, 116422. https://doi.org/10.1016/j.trac.2021.116422.

(13) Sarrut, M.; Corgier, A.; Crétier, G.; Le Masle, A.; Dubant, S.; Heinisch, S. Potential and Limitations of On-Line Comprehensive Reversed Phase Liquid Chromatography×supercritical Fluid Chromatography for the Separation of Neutral Compounds: An Approach to Separate an Aqueous Extract of Bio-Oil. *J. Chromatogr. A* **2015**, *1402*, 124–133. https://doi.org/10.1016/j.chroma.2015.05.005.

(14) Nijssen, R.; Blokland, M. H.; Wegh, R. S.; de Lange, E.; van Leeuwen, S. P. J.; Berendsen, B. J. A.; van de Schans, M. G. M. Comparison of Compound Identification Tools Using Data Dependent and Data Independent High-Resolution Mass Spectrometry Spectra. *Metabolites* **2023**, *13* (7), 777. https://doi.org/10.3390/metabo13070777.

(15) Caño-Carrillo, I.; Gilbert-López, B.; Montero, L.; Martínez-Piernas, A. B.; García-Reyes, J. F.; Molina-Díaz, A. Comprehensive and Heart-Cutting Multidimensional Liquid Chromatography–Mass Spectrometry and Its Applications in Food Analysis. *Mass Spectrom. Rev. n/a* (n/a). https://doi.org/10.1002/mas.21845.
(16) Tsugawa, H.; Cajka, T.; Kind, T.; Ma, Y.; Higgins, B.; Ikeda, K.; Kanazawa, M.; VanderGheynst, J.; Fiehn, O.; Arita, M. MS-DIAL: Data-Independent MS/MS Deconvolution for Comprehensive Metabolome Analysis. *Nat. Methods* **2015**, *12* (6), 523–526. https://doi.org/10.1038/nmeth.3393.
(17) Wang, M.; Carver, J. J.; Phelan, V. V.; Sanchez, L. M.; Garg, N.; Peng, Y.; Nguyen, D. D.; Watrous, J.; Kapono, C. A.; Luzzatto-Knaan, T.; Porto, C.; Bouslimani, A.; Melnik, A. V.; Meehan, M. J.; Liu, W.-T.; Crüsemann, M.; Boudreau, P. D.; Esquenazi, E.; Sandoval-Calderón, M.; Kersten, R. D.; Pace, L. A.; Quinn, R. A.; Duncan, K. R.; Hsu, C.-C.; Floros, D. J.; Gavilan, R. G.; Kleigrewe, K.; Northen, T.; Dutton, R. J.; Parrot, D.; Carlson, E. E.; Aigle, B.; Michelsen, C. F.; Jelsbak, L.; Sohlenkamp, C.; Pevzner, P.; Edlund, A.; McLean, J.; Piel, J.; Murphy, B. T.; Gerwick, L.; Liaw, C.-C.; Yang, Y.-L.; Humpf, H.-U.; Maansson, M.; Keyzers, R. A.; Sims, A. C.; Johnson, A. R.; Sidebottom, A. M.; Sedio, B. E.; Klitgaard, A.; Larson, C. B.; Boya P, C. A.; Torres-Mendoza, D.; Gonzalez, D. J.; Silva, D. B.; Marques, L. M.; Demarque, D. P.; Pociute, E.; O'Neill, E. C.; Briand, E.; Helfrich, E. J. N.; Granatosky, E. A.; Glukhov, E.; Ryffel, F.; Houson, H.; Mohimani, H.; Kharbush, J. J.; Zeng, Y.; Vorholt, J. A.; Kurita, K. L.; Charusanti, P.; McPhail, K. L.; Nielsen, K. F.; Vuong, L.; Elfeki, M.; Traxler, M. F.; Engene, N.; Koyama, N.; Vining, O. B.; Baric, R.; Silva, R. R.; Mascuch, S. J.; Tomasi, S.; Jenkins, S.; Macherla, V.; Hoffman, T.; Agarwal, V.; Williams, P. G.; Dai, J.; Neupane, R.; Gurr, J.; Rodríguez, A. M. C.; Lamsa, A.; Zhang, C.; Dorrestein, K.; Duggan, B. M.; Almaliti, J.; Allard, P.-M.; Phapale, P.; Nothias, L.-F.; Alexandrov, T.; Litaudon, M.; Wolfender, J.-L.; Kyle, J. E.; Metz, T. O.; Peryea, T.; Nguyen, D.-T.; VanLeer, D.; Shinn, P.; Jadhav, A.; Müller, R.; Waters, K. M.; Shi, W.; Liu, X.; Zhang, L.; Knight, R.; Jensen, P. R.; Palsson, B. Ø.; Pogliano, K.; Linington, R. G.; Gutiérrez, M.; Lopes, N. P.; Gerwick, W. H.; Moore, B. S.; Dorrestein, P. C.; Bandeira, N. Sharing and Community Curation of Mass Spectrometry Data with Global Natural Products Social Molecular Networking. *Nat. Biotechnol.* **2016**, *34* (8), 828–837. https://doi.org/10.1038/nbt.3597.
(18) Olivon, F.; Apel, C.; Retailleau, P.; M. Allard, P.; L. Wolfender, J.; Touboul, D.; Roussi, F.; Litaudon, M.; Desrat, S. Searching for Original Natural Products by Molecular Networking: Detection, Isolation and Total Synthesis of Chloroaustralasines. *Org. Chem. Front.* **2018**, *5* (14), 2171–2178. https://doi.org/10.1039/C8QO00429C.
(19) Pan, H.; Zhou, H.; Miao, S.; Cao, J.; Liu, J.; Lan, L.; Hu, Q.; Mao, X.; Ji, S. An Integrated Approach for Global Profiling of Multi-Type Constituents: Comprehensive Chemical Characterization of Lonicerae Japonicae Flos as a Case Study. *J. Chromatogr. A* **2020**, *1613*, 460674. https://doi.org/10.1016/j.chroma.2019.460674.
(20) Wang, M.; Xu, X.; Wang, H.; Wang, H.; Liu, M.; Hu, W.; Chen, B.; Jiang, M.; Qi, J.; Li, X.; Yang, W.; Gao, X. A Multi-Dimensional Liquid Chromatography/High-Resolution Mass Spectrometry Approach Combined with Computational Data Processing for the Comprehensive Characterization of the Multicomponents from Cuscuta Chinensis. *J. Chromatogr. A* **2022**, *1675*, 463162. https://doi.org/10.1016/j.chroma.2022.463162.
(21) Zhang, Z.; Xu, Y.; Shen, A.; Fu, D.; Liu, D.; Liu, Y.; Liang, X. Offline Two-Dimensional Normal-Phase × Reversed-Phase Liquid Chromatography Coupled with High-Resolution Mass Spectrometry for Comprehensive Analysis of Chemical Constituents in Euphorbia Kansui. *J. Chromatogr. A* **2023**, *1693*, 463897. https://doi.org/10.1016/j.chroma.2023.463897.
(22) Dai, Y.; Zhang, K.; Xiong, L.; Wang, L.; Guo, Z.; Yang, J.; Wu, A.; Wu, J.; Zeng, J. Comprehensive Profiling of Sanguisorba Officinalis Using Offline Two-Dimensional Mixed-Mode Liquid Chromatography × Reversed-Phase Liquid Chromatography, Tandem High-Resolution Mass Spectrometry, and Molecular Network. *J. Sep. Sci.* **2022**, *45* (10), 1727–1736. https://doi.org/10.1002/jssc.202200013.
(23) Qu, B.; Liu, Y.; Shen, A.; Guo, Z.; Yu, L.; Liu, D.; Huang, F.; Peng, T.; Liang, X. Combining Multidimensional Chromatography-Mass Spectrometry and Feature-Based Molecular Networking Methods for the Systematic Characterization of Compounds in the Supercritical Fluid Extract of Tripterygium Wilfordii Hook F. *Analyst* **2023**, *148* (1), 61–73. https://doi.org/10.1039/D2AN01471H.

(24) Wei, W.; Hou, J.; Yao, C.; Bi, Q.; Wang, X.; Li, Z.; Jin, Q.; Lei, M.; Feng, Z.; Wu, W.; Guo, D. A High-Efficiency Strategy Integrating Offline Two-Dimensional Separation and Data Post-Processing with Dereplication: Characterization of Bufadienolides in Venenum Bufonis as a Case Study. *J. Chromatogr. A* **2019**, *1603*, 179–189. https://doi.org/10.1016/j.chroma.2019.06.037.
(25) Teboul, E.; Tammekivi, E.; Batteau, M.; Geantet, C.; Faure, K. Off-Line Two-Dimensional Separation Involving Supercritical Fluid Chromatography for the Characterization of the Wastewater from Algae Hydrothermal Liquefaction. *J. Chromatogr. A* **2023**, *1694*, 463907. https://doi.org/10.1016/j.chroma.2023.463907.
(26) Sipilä, K.; Kuoppala, E.; Fagernäs, L.; Oasmaa, A. Characterization of Biomass-Based Flash Pyrolysis Oils. *Biomass Bioenergy* **1998**, *14* (2), 103–113. https://doi.org/10.1016/S0961-9534(97)10024-1.
(27) Branca, C.; Giudicianni, P.; Di Blasi, C. GC/MS Characterization of Liquids Generated from Low-Temperature Pyrolysis of Wood. *Ind. Eng. Chem. Res.* **2003**, *42* (14), 3190–3202. https://doi.org/10.1021/ie030066d.
(28) Le Masle, A.; Angot, D.; Gouin, C.; D'Attoma, A.; Ponthus, J.; Quignard, A.; Heinisch, S. Development of On-Line Comprehensive Two-Dimensional Liquid Chromatography Method for the Separation of Biomass Compounds. *J. Chromatogr. A* **2014**, *1340*, 90–98. https://doi.org/10.1016/j.chroma.2014.03.020.
(29) Guillarme, D.; Desfontaine, V.; Heinisch, S.; Veuthey, J.-L. What Are the Current Solutions for Interfacing Supercritical Fluid Chromatography and Mass Spectrometry? *J. Chromatogr. B* **2018**, *1083*, 160–170. https://doi.org/10.1016/j.jchromb.2018.03.010.
(30) Tsugawa, H.; Kind, T.; Nakabayashi, R.; Yukihira, D.; Tanaka, W.; Cajka, T.; Saito, K.; Fiehn, O.; Arita, M. Hydrogen Rearrangement Rules: Computational MS/MS Fragmentation and Structure Elucidation Using MS-FINDER Software. *Anal. Chem.* **2016**, *88* (16), 7946–7958. https://doi.org/10.1021/acs.analchem.6b00770.
(31) Montero, L.; Meckelmann, S. W.; Kim, H.; Ayala-Cabrera, J. F.; Schmitz, O. J. Differentiation of Industrial Hemp Strains by Their Cannabinoid and Phenolic Compounds Using LC × LC-HRMS. *Anal. Bioanal. Chem.* **2022**, *414* (18), 5445–5459. https://doi.org/10.1007/s00216-022-03925-8.
(32) Nothias, L.-F.; Petras, D.; Schmid, R.; Dührkop, K.; Rainer, J.; Sarvepalli, A.; Protsyuk, I.; Ernst, M.; Tsugawa, H.; Fleischauer, M.; Aicheler, F.; Aksenov, A. A.; Alka, O.; Allard, P.-M.; Barsch, A.; Cachet, X.; Caraballo-Rodriguez, A. M.; Da Silva, R. R.; Dang, T.; Garg, N.; Gauglitz, J. M.; Gurevich, A.; Isaac, G.; Jarmusch, A. K.; Kameník, Z.; Kang, K. B.; Kessler, N.; Koester, I.; Korf, A.; Le Gouellec, A.; Ludwig, M.; Martin H., C.; McCall, L.-I.; McSayles, J.; Meyer, S. W.; Mohimani, H.; Morsy, M.; Moyne, O.; Neumann, S.; Neuweger, H.; Nguyen, N. H.; Nothias-Esposito, M.; Paolini, J.; Phelan, V. V.; Pluskal, T.; Quinn, R. A.; Rogers, S.; Shrestha, B.; Tripathi, A.; van der Hooft, J. J. J.; Vargas, F.; Weldon, K. C.; Witting, M.; Yang, H.; Zhang, Z.; Zubeil, F.; Kohlbacher, O.; Böcker, S.; Alexandrov, T.; Bandeira, N.; Wang, M.; Dorrestein, P. C. Feature-Based Molecular Networking in the GNPS Analysis Environment. *Nat. Methods* **2020**, *17* (9), 905–908. https://doi.org/10.1038/s41592-020-0933-6.
(33) Dührkop, K.; Fleischauer, M.; Ludwig, M.; Aksenov, A. A.; Melnik, A. V.; Meusel, M.; Dorrestein, P. C.; Rousu, J.; Böcker, S. SIRIUS 4: A Rapid Tool for Turning Tandem Mass Spectra into Metabolite Structure Information. *Nat. Methods* **2019**, *16* (4), 299–302. https://doi.org/10.1038/s41592-019-0344-8.
(34) Böcker, S.; Dührkop, K. Fragmentation Trees Reloaded. *J. Cheminformatics* **2016**, *8* (1), 5. https://doi.org/10.1186/s13321-016-0116-8.
(35) Dührkop, K.; Shen, H.; Meusel, M.; Rousu, J.; Böcker, S. Searching Molecular Structure Databases with Tandem Mass Spectra Using CSI:FingerID. *Proc. Natl. Acad. Sci.* **2015**, *112* (41), 12580–12585. https://doi.org/10.1073/pnas.1509788112.
(36) Djoumbou Feunang, Y.; Eisner, R.; Knox, C.; Chepelev, L.; Hastings, J.; Owen, G.; Fahy, E.; Steinbeck, C.; Subramanian, S.; Bolton, E.; Greiner, R.; Wishart, D. S. ClassyFire: Automated Chemical Classification with a Comprehensive, Computable Taxonomy. *J. Cheminformatics* **2016**, *8* (1), 61. https://doi.org/10.1186/s13321-016-0174-y.
(37) Kim, H. W.; Wang, M.; Leber, C. A.; Nothias, L.-F.; Reher, R.; Kang, K. B.; van der Hooft, J. J. J.; Dorrestein, P. C.; Gerwick, W. H.; Cottrell, G. W. NPClassifier: A Deep Neural Network-

Based Structural Classification Tool for Natural Products. *J. Nat. Prod.* **2021**, *84* (11), 2795–2807. https://doi.org/10.1021/acs.jnatprod.1c00399.
(38) Dührkop, K.; Nothias, L.-F.; Fleischauer, M.; Reher, R.; Ludwig, M.; Hoffmann, M. A.; Petras, D.; Gerwick, W. H.; Rousu, J.; Dorrestein, P. C.; Böcker, S. Systematic Classification of Unknown Metabolites Using High-Resolution Fragmentation Mass Spectra. *Nat. Biotechnol.* **2021**, *39* (4), 462–471. https://doi.org/10.1038/s41587-020-0740-8.
(39) Li, X.; Stoll, D. R.; Carr, P. W. Equation for Peak Capacity Estimation in Two-Dimensional Liquid Chromatography. *Anal. Chem.* **2009**, *81* (2), 845–850. https://doi.org/10.1021/ac801772u.
(40) Semard, G.; Peulon-Agasse, V.; Bruchet, A.; Bouillon, J.-P.; Cardinaël, P. Convex Hull: A New Method to Determine the Separation Space Used and to Optimize Operating Conditions for Comprehensive Two-Dimensional Gas Chromatography. *J. Chromatogr. A* **2010**, *1217* (33), 5449–5454. https://doi.org/10.1016/j.chroma.2010.06.048.
(41) Prothmann, J.; Sun, M.; Spégel, P.; Sandahl, M.; Turner, C. Ultra-High-Performance Supercritical Fluid Chromatography with Quadrupole-Time-of-Flight Mass Spectrometry (UHPSFC/QTOF-MS) for Analysis of Lignin-Derived Monomeric Compounds in Processed Lignin Samples. *Anal. Bioanal. Chem.* **2017**, *409* (30), 7049–7061. https://doi.org/10.1007/s00216-017-0663-5.
(42) Prothmann, J.; Palmer, S.; Turner, C.; Sandahl, M. Separation of Monomeric and Dimeric Phenolic Compounds in Lignosulphonate Lignin on Different Stationary Phases Using Ultrahigh-Performance Supercritical Fluid Chromatography. *J. Chromatogr. A* **2021**, *1653*, 462408. https://doi.org/10.1016/j.chroma.2021.462408.
(43) Guo, J.; Huan, T. Turning Metabolomics Data Processing from a “Black Box” to a “White Box.” *LCGC Suppl.* **2022**, *40* (s9), 20–22.
(44) Xu, Y.-F.; Lu, W.; Rabinowitz, J. D. Avoiding Misannotation of In-Source Fragmentation Products as Cellular Metabolites in Liquid Chromatography–Mass Spectrometry-Based Metabolomics. *Anal. Chem.* **2015**, *87* (4), 2273–2281. https://doi.org/10.1021/ac504118y.
(45) Wasito, H.; Causon, T.; Hann, S. Alternating In-Source Fragmentation with Single-Stage High-Resolution Mass Spectrometry with High Annotation Confidence in Non-Targeted Metabolomics. *Talanta* **2022**, *236*, 122828. https://doi.org/10.1016/j.talanta.2021.122828.
(46) Tada, I.; Chaleckis, R.; Tsugawa, H.; Meister, I.; Zhang, P.; Lazarinis, N.; Dahlén, B.; Wheelock, C. E.; Arita, M. Correlation-Based Deconvolution (CorrDec) To Generate High-Quality MS2 Spectra from Data-Independent Acquisition in Multisample Studies. *Anal. Chem.* **2020**, *92* (16), 11310–11317. https://doi.org/10.1021/acs.analchem.0c01980.
(47) Jumaah, F.; Plaza, M.; Abrahamsson, V.; Turner, C.; Sandahl, M. A Fast and Sensitive Method for the Separation of Carotenoids Using Ultra-High Performance Supercritical Fluid Chromatography-Mass Spectrometry. *Anal. Bioanal. Chem.* **2016**, *408* (21), 5883–5894. https://doi.org/10.1007/s00216-016-9707-5.
(48) Smith, C. J.; Perfetti, T. A.; Morton, M. J.; Rodgman, A.; Garg, R.; Selassie, C. D.; Hansch, C. The Relative Toxicity of Substituted Phenols Reported in Cigarette Mainstream Smoke. *Toxicol. Sci.* **2002**, *69* (1), 265–278. https://doi.org/10.1093/toxsci/69.1.265.
(49) Schymanski, E. L.; Jeon, J.; Gulde, R.; Fenner, K.; Ruff, M.; Singer, H. P.; Hollender, J. Identifying Small Molecules via High Resolution Mass Spectrometry: Communicating Confidence. *Environ. Sci. Technol.* **2014**, *48* (4), 2097–2098. https://doi.org/10.1021/es5002105.
(50) Karatt, T. K.; Nalakath, J.; Perwad, Z.; Albert, P. H.; Abdul Khader, K. K.; Syed Ali Padusha, M.; Laya, S. Mass Spectrometric Method for Distinguishing Isomers of Dexamethasone via Fragment Mass Ratio: An HRMS Approach. *J. Mass Spectrom.* **2018**, *53* (11), 1046–1058. https://doi.org/10.1002/jms.4279.
(51) Koelmel, J. P.; Li, X.; Stow, S. M.; Sartain, M. J.; Murali, A.; Kemperman, R.; Tsugawa, H.; Takahashi, M.; Vasiliou, V.; Bowden, J. A.; Yost, R. A.; Garrett, T. J.; Kitagawa, N. Lipid Annotator: Towards Accurate Annotation in Non-Targeted Liquid Chromatography High-Resolution Tandem Mass Spectrometry (LC-HRMS/MS) Lipidomics Using a Rapid and User-Friendly Software. *Metabolites* **2020**, *10* (3), 101. https://doi.org/10.3390/metabo10030101.
(52) Menicatti, M.; Pallecchi, M.; Bua, S.; Vullo, D.; Di Cesare Mannelli, L.; Ghelardini, C.; Carta, F.; Supuran, C. T.; Bartolucci, G. Resolution of Co-Eluting Isomers of Anti-Inflammatory Drugs Conjugated to Carbonic Anhydrase Inhibitors from Plasma in Liquid Chromatography by Energy-

Resolved Tandem Mass Spectrometry. *J. Enzyme Inhib. Med. Chem.* **2018**, *33* (1), 671–679. https://doi.org/10.1080/14756366.2018.1445737.
(53) Pua, A.; Goh, R. M. V.; Ee, K.-H.; Huang, Y.; Liu, S. Q.; Lassabliere, B.; Yu, B. Improving Resolution of Isomeric Flavonoids and Their Glycosides Using Two-Dimensional Liquid Chromatography Coupled With High-Resolution Mass Spectrometry. *Chromatographia* **2021**, *84* (5), 507–515. https://doi.org/10.1007/s10337-021-04027-w.
(54) Ganzera, M.; Zwerger, M. Analysis of Natural Products by SFC – Applications from 2015 to 2021. *TrAC Trends Anal. Chem.* **2021**, *145*, 116463. https://doi.org/10.1016/j.trac.2021.116463.